Background Noise Reduction of Attention Map for Weakly Supervised Semantic Segmentation

Izumi Fujimori¹, Masaki Oono¹, Masami Shishibori¹ ¹Tokushima University

{Izumi Fujimori}c612435027@tokushima-u.ac.jp

Abstract

In weakly-supervised semantic segmentation (WSSS) using only image-level class labels, a problem with CNNbased Class Activation Maps (CAM) is that they tend to activate the most discriminative local regions of objects. On the other hand, methods based on Transformers learn global features but suffer from the issue of background noise contamination. This paper focuses on addressing the issue of background noise in attention weights within the existing WSSS method based on Conformer. known as TransCAM. The proposed method successfully reduces background noise, leading to improved accuracy of pseudo labels. Experimental results demonstrate that our model achieves segmentation performance of 70.5% on the PAS-CAL VOC 2012 validation data, 71.1% on the test data, and 45.9% on MS COCO 2014 data, outperforming TransCAM in terms of segmentation performance.

1. Introduction

Semantic Segmentation is a fundamental task in computer vision, becoming increasingly important in a wide range of applications such as autonomous driving and land cover classification. While traditional supervised semantic segmentation methods have yielded excellent results^[2]^[27], they demand extensive labeled data for training, making annotation efforts a significant hurdle. To tackle this challenge, Weakly-Supervised Semantic Segmentation (WSSS) has emerged. WSSS aims to reduce annotation costs by utilizing annotation information other than pixel-level annotations. Various methods have been proposed in the realm of WSSS, including bounding boxes[21], scribbles[24], and points[3]. Among these, the most costeffective approach involves utilizing only image-level class This method leverages label information from labels. predicted classes for the entire image to assign class labels to individual pixels. Image-level class labels are easily obtainable from existing large-scale datasets such

as ImageNet[31], substantially reducing annotation costs. This paper focuses on WSSS using image-level class labels and proposes a method to enhance its segmentation accuracy.

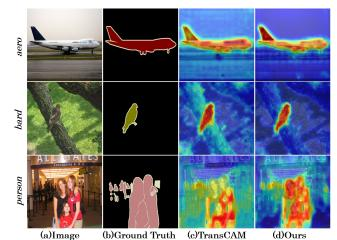


Figure 1: Comparison of CAMs generated by TransCAM and our proposed method. (a)Input image, (b)Ground Truth, (c)TransCAM, (d)CAMs by our method.

In recent years, methods for WSSS have seen remarkable advancements. A common approach in WSSS involves generating pseudo labels using Class Activation Maps^[42] (CAM) based on Convolutional Neural Networks (CNNs). However, since CNNs learn features locally, the generated CAMs tend to activate only parts of objects intensely. Vision Transformer[8] (ViT), based on Transformer[33] models with Multi-Head Self-Attention (MHSA), has brought breakthroughs in image recognition tasks. It has also been applied to WSSS, with methods utilizing attention maps to represent global features. However, issues such as background noise contamination and mislabeling of classes Background noise degrades the performance of arise. CAMs. Therefore, this approach proposes a method to reduce background noise. It is composed of Conformers[30]. aiming to alleviate background noise in WSSS. In the WSSS method based on Conformer called TransCAM[23],

CAM obtained from CNN is enhanced using attention maps obtained from ViT. During model training, both the CAM based on CNN and the class tokens output from ViT are fed into the loss function. In addition to CAM and class tokens, the proposed method inputs CAM enhanced with attention maps into the loss function to reduce background noise. By incorporating the CAM enhanced with attention maps into the loss function, the training progresses in a direction where background noise is reduced. Figure 1 illustrates CAM generated by the proposed method compared to CAM generated by existing methods, showing a reduction in background noise in the proposed method. In experiments using the PASCAL VOC 2012 dataset[9], the segmentation performance was 70.5% for the validation data and 71.1% for the test data. For experiments using the MS COCO 2014 dataset[25], the performance was 45.9%. The main contributions of this study are as follows:

- Proposing a method to input CAM enhanced with attention maps into the loss function during training, which reduces background noise derived from attention.
- Conducting experiments on PASCAL VOC 2012 and MS COCO 2014 datasets, achieving segmentation accuracy surpassing existing methods.

2. Related Work

2.1. Weakly supervised semantic segmentation based on CNN

Research on generating pseudo labels in WSSS has been a critical endeavor for improving the accuracy of segmentation tasks. A common approach involves utilizing Class Activation Maps (CAMs) from CNN classification networks to generate pseudo labels, which are then used as training data for supervised segmentation learning. However, CAMs suffer from the issue of activating only localized regions of the target. In recent years, research focusing on addressing the problem of localized activation in CAMs has advanced. SEC[15] extends the heat range of CAMs by expanding seed regions. Adversarial erasing[35] removes highly discriminative regions of objects, activating the remaining less discriminative regions. SEAM[34] applies consistency regularization to CAMs predicted from images subjected to affine transformations. Additionally, it proposes a Pixel Correlation Module to enhance CAM consistency. Hide-and-Seek[17] randomly hides patches in images during training, prompting the network to explore other relevant parts. CPN[41] divides images into complementary patches for a more comprehensive seed region in CAMs. PSA[1] learns a network to predict semantic affinity matrices between pairs of adjacent image coordinates and propagates semantic affinity matrices using random walk[29]. Despite many excellent improvements, CNN-based methods still have limitations in representing global features.

2.2. Weakly supervised semantic segmentation based on Transformer

The breakthrough achieved by Vision Transformer (ViT) in image recognition tasks has also been applied to WSSS. Excellent methods leveraging the advantage of Transformer in capturing global features have been proposed. TS-CAM[10] generates pseudo labels using patch tokens and attention maps. MCTformer+[37] enhances class token discriminability by proposing the Contrastive Class Tokens Module, which multiplies class tokens. WeakTr[43] estimates the importance of attention weights used to enhance CAMs and proposes the Adaptive Attention Fusion Module to allocate weights adaptively. Efforts have also been made to utilize a Conformer[30] with a dual-branch structure of CNN and ViT as the backbone network. TransCAM[23] is pioneering research that applies Conformer as the backbone network to the WSSS task, enhancing CAMs from the CNN branch with attention maps. MECPformer[26] utilizes a Conformer backbone network and transforms images into complementary patches inspired by CPN[41]. It learns multiple estimation complementary patches across different learning epochs to reduce false detections. He et al^[12] pointed out the phenomenon of excessive smoothing of attention weights causing irrelevant background noise and proposed the Adaptive Re-activation Mechanism With Affinity Matrix. By learning to make the affinity matrices derived from pseudo labels closer to the values of attention weights, excessive smoothing of attention weights is mitigated. This paper proposes a method to alleviate background noise in attention maps by inputting CAMs enhanced with attention maps into the loss function for training.

3. Methodology

Figure 2 illustrates an overview of the proposed method. The backbone network is composed of the Conformer architecture. Refined feature maps enhanced by attention maps are augmented with the noise \overline{A}^* . Next, the feature maps with added noise are fed into the loss function. Pseudo-labels are generated from seeds with reduced background noise.

3.1. Conformer as the backbone

In this method, a Conformer serves as the backbone network. The Conformer adopts a hybrid structure comprising CNN-block and Transformer-block. The CNN-block is based on ResNet[13], while the Transformer-block is inspired by ViT[8]. The Conformer utilizes Feature Coupling Unit[30] (FCU) to integrate the local features learned by the CNN-block with the global features learned by the Transformer-block.

3.2. Seed generation

CAM generation. Let's denote the output of the last CNN-block as $f \in \mathbb{R}^{fc \times fh \times fw}$, where fc, fh and fw represent the number of channels, height, and width of the feature map, respectively. The weight corresponding to the feature map of the final layer is represented as $w \in \mathbb{R}^{fc}$. We denote the CAM as $M \in \mathbb{R}^{S \times fh \times fw}$, where S represents the number of classes. The CAM corresponding to the s-th class $M_s \in \mathbb{R}^{fh \times fw}$ can be formulated as follows, where s represents a specific class:

$$M_s = w^\top f \tag{1}$$

The CAM generated from the CNN-block of the Conformer is designed to have a shape of $M_s \in \mathbb{R}^{\sqrt{N} \times \sqrt{N}}$, where N represents the size of the patch token.

Attention map generation. Let the attention weights obtained from the Transformer-block be represented as $A^{b,h} \in \mathbb{R}^{b \times h \times (1+N) \times (1+N)}$, where *b*, *h* and 1 denote a specific block, a specific head, and the class token, respectively. $A^{b,h}$ is computed using the following equation:

$$A^{b,h} = \operatorname{softmax}(\frac{Q^{b,h}K^{b,h\top}}{\sqrt{D/h}})$$
(2)

In the above equation, $Q^{b,h}$ and $K^{b,h}$ represent the queries and keys obtained in the *b*-th Transformer block, and *D* denotes the embedding dimensions of tokens. By averaging the attention weights $A^{b,h}$ across heads for each block, we obtain $\bar{A}^b \in \mathbb{R}^{b \times (1+N) \times (1+N)}$, computed as follows:

$$\bar{A}^b = \frac{1}{H} \sum_h (A^{b,h}) \tag{3}$$

where H represents the number of heads. Summing \bar{A}^b across layers yields a single attention weight calculated from the attention weights of each block and each head. This yields $A \in \mathbb{R}^{(1+N) \times (1+N)}$, computed as:

$$A = \sum_{b} (\bar{A}^{b}) \tag{4}$$

In $A \in \mathbb{R}^{(1+N)\times(1+N)}$, removing the attention weights associated with the class token results in an attention map $A^* \in \mathbb{R}^{N \times N}$.

Refinement of CAM with Attention Map. Reshaping the CAM corresponding to the *s*-th class $M_s \in \mathbb{R}^{\sqrt{N} \times \sqrt{N}}$ into $M_s \in \mathbb{R}^{N \times 1}$, enhanced by the attention map $A^* \in \mathbb{R}^{N \times N}$, is calculated as follows:

$$M_s^{\ *} = A^* \cdot M_s \tag{5}$$

where $M_s^* \in \mathbb{R}^{N \times 1}$, which is then reshaped into $M_s^* \in \mathbb{R}^{\sqrt{N} \times \sqrt{N}}$. M_s^* is considered as the inference result. Consequently, $M^* \in \mathbb{R}^{S \times \sqrt{N} \times \sqrt{N}}$.

3.3. Background noise reduction and training

Enhanced CAMs $M_s^* \in \mathbb{R}^{N \times 1}$, bolstered by attention maps, are not directly utilized in the loss function and thus do not contribute to the network's learning process. Consequently, it is presumed that M_s^* may contain superfluous background noise. To address this, our method proposes monitoring M_s^* by inputting it into the Multi-label Soft Margin Loss during training, thereby alleviating background noise. Furthermore, augmenting M_s^* with noise $\bar{A}^* \in \mathbb{R}^{N \times N}$ during training proves to be effective. The noise added to M_s^* is denoted by M_s^{**} . This noise addition is done as follows:

$$M_s^{**} = \bar{A}^* \cdot M_s^* \tag{6}$$

where, $M_s^{**} \in \mathbb{R}^{N \times 1}$, which is then reshaped into $M_s^{**} \in \mathbb{R}^{\sqrt{N} \times \sqrt{N}}$. The noise $\bar{A}^* \in \mathbb{R}^{N \times N}$ is obtained by averaging the attention weights relevant to the class token in \bar{A}^b , calculated by averaging $\bar{A} \in \mathbb{R}^{(1+N) \times (1+N)}$ along the layer direction in Equation 3. \bar{A} is computed as follows:

$$\bar{A} = \frac{1}{B} \sum_{b} (\bar{A}^{b}) \tag{7}$$

where, *B* represents the number of blocks. \overline{A}^* is only added as noise during training. By applying Global Average Pooling (GAP) to the CAM augmented with noise, $M^{**} \in \mathbb{R}^{S \times \sqrt{N} \times \sqrt{N}}$, we obtain $z \in \mathbb{R}^S$. We can then compute the multi-label soft margin loss $L_{M^{**}}$ for z using the following equation:

$$L_{M^{**}} = -\frac{1}{S-1} \sum_{s=1}^{S-1} [y_s \ln(\frac{1}{1+\exp(-z_s)}) + (1-y_s) \ln(\frac{\exp(-z_s)}{1+\exp(-z_s)})]$$
(8)

where, $y_s \in \{0, 1\}$ represents the ground truth for class s, and $z_s \in \mathbb{R}$ is the classification prediction for class s. Additionally, we add the value obtained by applying a linear layer to $M \in \mathbb{R}^{S \times \sqrt{N} \times \sqrt{N}}$ after applying GAP and the class token, $t \in \mathbb{R}^{(1+N) \times D}$, and input the resulting value into Equation 8 to obtain the loss L_{cls} . where, D represents the embedding dimensions of tokens. We train using the following loss equation:

$$L = L_{cls} + L_{M^{**}} \tag{9}$$

During inference, \bar{A}^* is not included as noise. Inference follows the same method as TransCAM (Baseline).

3.4. Pseudo label generation

Pseudo-label Generation Enhanced CAMs $M_s^* \in \mathbb{R}^{\sqrt{N} \times \sqrt{N}}$, strengthened by attention maps, are normalized

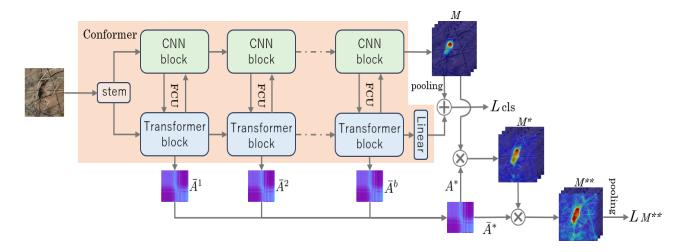


Figure 2: Overview of the proposed method. Create TransCAM from input images. Add noise to TransCAM and input it to the loss function. Train TransCAM using image-level lable. Attention map is explicitly incorporated into the training process to suppress the background noise derived from the Attention map. Pseudo-labels are created from the initial seed obtained from TransCAM. The trained TransCAM has reduced background noise.

within the range of [0, 1]. In this case, the class s range excludes the background class, defined as $1 \le s \le S - 1$. We establish a hard threshold ht = [0, 1]. For each pixel in the normalized CAM $M^* \in \mathbb{R}^{S \times \sqrt{N} \times \sqrt{N}}$, we assign the class s with the maximum value in the s direction as the pseudo-label. Pixels with values below the Hard Threshold ht are labeled as the background class, while those with values equal to or above ht are classified as the foreground class.

4. Experiments

4.1. Dataset and Evaluation Metric

For the evaluation dataset, we utilized the PASCAL VOC 2012 and MS COCO 2014 datasets. In the PASCAL VOC 2012 dataset, segmentation was conducted into 21 classes, including a background class and 20 foreground classes. Although the training, validation, and test datasets contain 1,464, 1,449, and 1,456 images, respectively, it's common to augment the training data with 10,582 images from the Semantic Boundary Dataset[11]. The MS COCO 2014 dataset involves segmentation into 81 classes, including a background class and 80 foreground classes, with 82,081 training images and 40,137 validation images. Evaluation on the training data was performed using 81,394 images with pixel-level ground truth labels. The mean Intersection over Union (mIoU) was employed as the evaluation metric.

4.2. Implementation Details

The experiments were conducted using the NVIDIA RTX A6000 (VRAM 48GB). We utilized a Conformer pretrained on ImageNet-1k[31] as the backbone network. AdamW[28] was employed as the optimizer with a learn-

ing rate of $5e^{-5}$ and a weight decay of $5e^{-4}$. During training, images were randomly resized within the range of [320, 640] and then cropped to a size of 512×512 . During inference, images resized to 256×256 , 512×512 , and 768×768 were input to the model. CAMs were generated at each scale, which were then resized to the original size and aggregated. By utilizing multi-scale processing, predictions with high mIoU accuracy could be achieved. For training on the PASCAL VOC 2012 dataset, we set the number of epochs to 22 and the batch size to 8. For the MS COCO 2014 dataset, we set the number of epochs to 10 and the batch size to 16. PSA[1] was employed for postprocessing of pseudo-labels. The pseudo-labels generated after post-processing were refined using CRF[16]. The supervised segmentation model was based on ResNet38[36] and DeepLab[4].

4.3. Experimental Results

Table 1: Comparison of mIoUs (%) for seed maps and pseudo-semantic masks of Baseline and the proposed method on the train set.

Method	VOC	COCO
TransCAM[23](Baseline)	64.9	46.2
Ours	66.2	47.4
TransCAM[23](Baseline)+ PSA[1]	70.2	48.7
Ours + PSA[1]	71.3	50.6

We evaluated the accuracy of initial pseudo-label assignment. Table 1 presents the experimental results conducted on the PASCAL VOC 2012 training data and MS COCO 2014 training data. For the PASCAL VOC 2012 training data, the proposed method achieved 66.2%, surpassing the



Figure 3: Qualitative segmentation results on the PASCAL VOC 2012 validation set. (a) Original images; (b) Ground truth; (c)Prediction of Ours.

Table 2: Performance of Categorical Semantic Partitioning on val set and test set in PASCAL VOC 2012.

						-					-											
Method	bkg	aero	bike	bird	boat	bottle	bus	car	cat	chair	cow	table	dog	horse	mbk	person	plant	sheep	sofa	train	tv	mIoU
TransCAM(Baseline)	91.3	81.9	35.4	84.7	67.6	67.9	87.5	80.5	86.5	31.4	73.9	52.5	84.0	74.9	74.6	79.0	44.7	84.1	47.0	78.4	46.6	69.3
ours	91.6	85.3	35.8	87.1	70.5	72.2	87.0	82.8	87.7	32.5	77.2	52.6	84.0	75.9	74.7	81.1	50.9	85.1	48.4	76.5	42.1	70.5
TransCAM(Baseline)	91.2	82.2	36.2	89.8	57.8	65.1	85.7	81.5	84.2	28.3	77.4	55.9	82.1	80.0	78.9	76.5	48.0	84.7	57.2	72.7	45.8	69.6
ours	91.6	85.0	36.1	89.7	58.9	67.9	86.1	82.8	86.8	30.6	81.0	60.5	82.6	81.3	79.7	79.4	56.9	85.5	59.3	71.2	41.1	71.1

Table 3: Comparison of mIoUs (%) of segmentation performance in PASCAL VOC. Backbone indicates network for semantic segmentation. I denotes image-level labels and S denotes saliency maps.

J 1				
Method	Backbone	Sup.	val	test
AuxSegNet[38]ICCV21	RN38	I+S	69.0	68.6
$L2G[14]_{CVPR22}$	RN38	I+S	72.0	73.0
MECPformer[26]Arxiv23	RN101	I+S	72.0	72.0
SEAM[34]CVPR20	RN38	Ι	64.5	65.7
CONTA[40]NIPS20	RN38	Ι	66.1	66.7
Kweon et al.[18]ICCV21	RN38	Ι	68.4	68.2
CDA[32]ICCV21	RN38	Ι	66.1	66.8
CPN[41]ICCV21	RN38	Ι	67.8	68.5
AdvCAM[19]CVPR21	RN101	Ι	68.1	68.0
AMN[22]CVPR22	RN101	Ι	70.7	70.6
W-OoD[20]CVPR22	RN38	Ι	70.7	70.1
SIPE[5]CVPR22	RN38	Ι	68.2	69.5
Yoon et al.[39]ECCV22	RN38	Ι	70.9	71.7
OCR[7]CVPR23	RN38	Ι	72.7	70.7
LPCAM[6]CVPR23	RN38	Ι	72.6	72.4
MCTformer+[37]Arxiv23	RN38	Ι	74.0	73.6
He et al.[12]Arxiv23	RN38	Ι	69.9	70.0
TransCAM[23]JVCI23	RN38	Ι	69.3	69.6
Ours	RN38	Ι	70.5	71.1

Baseline accuracy by 1.3 percentage points. On the MS COCO 2014 training data, the proposed method achieved 47.4%, surpassing the Baseline accuracy by 1.2 percentage points.

Next, we evaluated the performance of the pseudo-labels

Table 4: Comparison of mIoUs(%) for segmentation performance on MS COCO val set.

Method	Backbone	Sup.	val
AuxSegNet[38]ICCV21	RN38	I+S	33.9
L2G[14]CVPR22	RN101	I+S	44.2
MECPformer[26]Arxiv23	RN101	I+S	42.4
SEAM[34]CVPR20	RN38	Ι	31.9
CONTA[40]NIPS20	RN38	Ι	32.8
Kweon et al.[18]ICCV21	RN38	Ι	36.4
CDA[32]ICCV21	RN38	Ι	33.2
AdvCAM[19]CVPR21	RN101	Ι	44.4
AMN[22]CVPR22	RN101	Ι	44.7
SIPE[5]CVPR22	RN38	Ι	43.6
Yoon et al.[39]ECCV22	RN38	Ι	44.8
OCR[7]CVPR23	RN38	Ι	42.5
LPCAM[6]CVPR23	RN38	Ι	42.8
MCTformer+[37]Arxiv23	RN38	Ι	45.2
TransCAM[23]JVCI23	RN38	Ι	45.7
Ours	RN38	Ι	45.9

after post-processing. Table 1 shows the experimental results conducted on the PASCAL VOC 2012 training data and MS COCO 2014 training data. For the PASCAL VOC 2012 training data, the proposed method achieved 71.3%, surpassing the Baseline accuracy by 1.1 percentage points. On the MS COCO 2014 training data, the proposed method achieved 50.6%, surpassing the Baseline accuracy by 1.9 percentage points.

We conducted supervised learning using pseudo-labels as the training data. Table 2 presents the semantic segmentation results on the class-wise PASCAL VOC 2012 validation data. The proposed method outperformed existing methods in 17 out of 20 classes, demonstrating the effectiveness of suppressing background noise not only for specific classes but also for each class individually. Figure 3 illustrates the inference results of the segmentation model trained with pseudo-labels generated by the proposed method, showing the original image, ground truth, and the segmentation results obtained by the proposed method, respectively.

Table 3,4 presents the segmentation accuracy, where "Sup." in the middle column denotes image-level labels, and "S" represents saliency maps. For the PASCAL VOC 2012 validation data, the proposed method achieved 70.5%, surpassing the Baseline accuracy by 1.2 percentage points. On the test data, it achieved 71.1%, surpassing the Baseline accuracy by 1.5 percentage points. For the MS COCO 2014 validation data, it achieved 45.9%, surpassing the Baseline accuracy by 0.2 percentage points.

4.4. Investigating the Effects of Adding Noise

In this section, we investigate the impact of varying levels of noise $(\bar{A}^* \in \mathbb{R}^{N \times N})$ on the inference results. We conducted training by sequentially adding noise (\bar{A}^*) . Table 5 compares the initial pseudo-label mIoU based on the amount of noise, obtained from the PASCAL VOC 2012 training data. From left to right, it shows the Baseline, results trained without noise, results trained with noise multiplied by 1 $(\bar{A}^* \cdot 1)$, and results trained with noise multiplied by 2 $(\bar{A}^* \cdot 2)$. The accuracy of the training the effectiveness of training with added noise. The decrease in accuracy of the training results with ot he suppression of both background noise and the activation of object regions in the attention map.

Table 5: Comparison of performance for different amounts of noise in the initial pseudo-labels in the PASCAL VOC train set.

noise	Baseline[23]	without noise	$\bar{A}^* \cdot 1$	$\bar{A}^* \cdot 2$
train	64.9	62.4	66.2	65.3

Figure 4 illustrates the transition of mIoU based on the Hard Threshold of pseudo-labels in PASCAL VOC 2012. The vertical axis represents mIoU, while the horizontal axis represents the Hard Threshold. The black line represents the transition of mIoU for pseudo-labels generated by the Baseline, while the red, blue, and green lines represent the transition of mIoU for pseudo-labels generated by the proposed method. When CAM contains a lot of background noise, at low Hard Thresholds, the background noise becomes part of the object area, leading to performance degradation. The proposed method exhibits higher mIoU when

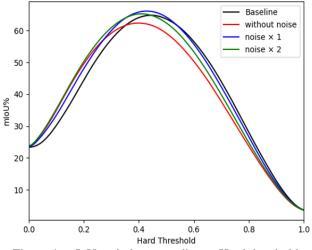


Figure 4: mIoU variation according to Hard thresholds

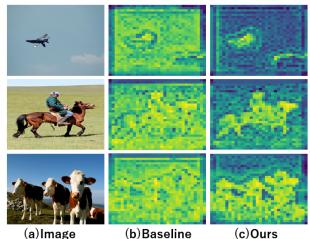


Figure 5: Comparisons of Attention map. (a) Original image; (b)Attention map generated by baseline; (c) Attention map generated by our method.

the Hard Threshold is lower than the Baseline, indicating a reduction in background noise.

Figure 5 compares the attention maps between the conventional method and the proposed method. It is evident that the activation of background regions is reduced in the attention maps generated by the proposed method compared to the conventional method.

5. Conclusion

This paper proposes a method to suppress background noise in attention maps by inputting attention mapenhanced CAMs into the loss function and evaluates its performance. The proposed method surpassed the accuracy of existing methods on the PASCAL VOC 2012 dataset and MS COCO 2014 dataset. Since the activation of object regions tended to be suppressed in the proposed method, future work could focus on designing loss functions aimed at suppressing background noise.

References

- Jiwoon Ahn and Suha Kwak. Learning pixel-level semantic affinity with image-level supervision for weakly supervised semantic segmentation. In *Proceedings of the IEEE conference on computer vision and pattern recognition*, pages 4981–4990, 2018. 2, 4
- [2] Vijay Badrinarayanan, Alex Kendall, and Roberto Cipolla. Segnet: A deep convolutional encoder-decoder architecture for image segmentation. *IEEE transactions on pattern analysis and machine intelligence*, 39(12):2481–2495, 2017. 1
- [3] Amy Bearman, Olga Russakovsky, Vittorio Ferrari, and Li Fei-Fei. What's the point: Semantic segmentation with point supervision. In *European conference on computer vision*, pages 549–565. Springer, 2016. 1
- [4] Liang-Chieh Chen, George Papandreou, Iasonas Kokkinos, Kevin Murphy, and Alan L Yuille. Semantic image segmentation with deep convolutional nets and fully connected crfs. arXiv preprint arXiv:1412.7062, 2014. 4
- [5] Qi Chen, Lingxiao Yang, Jian-Huang Lai, and Xiaohua Xie. Self-supervised image-specific prototype exploration for weakly supervised semantic segmentation. In *Proceedings of the IEEE/CVF Conference on Computer Vision and Pattern Recognition*, pages 4288–4298, 2022. 5
- [6] Zhaozheng Chen and Qianru Sun. Extracting class activation maps from non-discriminative features as well. In Proceedings of the IEEE/CVF Conference on Computer Vision and Pattern Recognition, pages 3135–3144, 2023. 5
- [7] Zesen Cheng, Pengchong Qiao, Kehan Li, Siheng Li, Pengxu Wei, Xiangyang Ji, Li Yuan, Chang Liu, and Jie Chen. Outof-candidate rectification for weakly supervised semantic segmentation. In *Proceedings of the IEEE/CVF Conference* on Computer Vision and Pattern Recognition, pages 23673– 23684, 2023. 5
- [8] Alexey Dosovitskiy, Lucas Beyer, Alexander Kolesnikov, Dirk Weissenborn, Xiaohua Zhai, Thomas Unterthiner, Mostafa Dehghani, Matthias Minderer, Georg Heigold, Sylvain Gelly, et al. An image is worth 16x16 words: Transformers for image recognition at scale. arXiv preprint arXiv:2010.11929, 2020. 1, 2
- [9] Mark Everingham, Luc Van Gool, Christopher KI Williams, John Winn, and Andrew Zisserman. The pascal visual object classes (voc) challenge. *International journal of computer vision*, 88:303–338, 2010. 2
- [10] Wei Gao, Fang Wan, Xingjia Pan, Zhiliang Peng, Qi Tian, Zhenjun Han, Bolei Zhou, and Qixiang Ye. Ts-cam: Token semantic coupled attention map for weakly supervised object localization. In *Proceedings of the IEEE/CVF International Conference on Computer Vision*, pages 2886–2895, 2021. 2
- [11] Bharath Hariharan, Pablo Arbeláez, Lubomir Bourdev, Subhransu Maji, and Jitendra Malik. Semantic contours from inverse detectors. In 2011 international conference on computer vision, pages 991–998. IEEE, 2011. 4
- [12] Jingxuan He, Lechao Cheng, Chaowei Fang, Dingwen Zhang, Zhangye Wang, and Wei Chen. Mitigating undisciplined over-smoothing in transformer for weakly supervised

semantic segmentation. *arXiv preprint arXiv:2305.03112*, 2023. 2, 5

- [13] Kaiming He, Xiangyu Zhang, Shaoqing Ren, and Jian Sun. Deep residual learning for image recognition. In *Proceed-ings of the IEEE conference on computer vision and pattern recognition*, pages 770–778, 2016. 2
- [14] Peng-Tao Jiang, Yuqi Yang, Qibin Hou, and Yunchao Wei. L2g: A simple local-to-global knowledge transfer framework for weakly supervised semantic segmentation. In Proceedings of the IEEE/CVF conference on computer vision and pattern recognition, pages 16886–16896, 2022. 5
- [15] Alexander Kolesnikov and Christoph H Lampert. Seed, expand and constrain: Three principles for weakly-supervised image segmentation. In *Computer Vision–ECCV 2016: 14th European Conference, Amsterdam, The Netherlands, October 11–14, 2016, Proceedings, Part IV 14*, pages 695–711. Springer, 2016. 2
- Philipp Krähenbühl and Vladlen Koltun. Efficient inference in fully connected crfs with gaussian edge potentials. Advances in neural information processing systems, 24, 2011.
 4
- [17] Krishna Kumar Singh and Yong Jae Lee. Hide-and-seek: Forcing a network to be meticulous for weakly-supervised object and action localization. In *Proceedings of the IEEE International Conference on Computer Vision*, pages 3524– 3533, 2017. 2
- [18] Hyeokjun Kweon, Sung-Hoon Yoon, Hyeonseong Kim, Daehee Park, and Kuk-Jin Yoon. Unlocking the potential of ordinary classifier: Class-specific adversarial erasing framework for weakly supervised semantic segmentation. In *Proceedings of the IEEE/CVF international conference on computer vision*, pages 6994–7003, 2021. 5
- [19] Jungbeom Lee, Eunji Kim, Jisoo Mok, and Sungroh Yoon. Anti-adversarially manipulated attributions for weakly supervised semantic segmentation and object localization. *IEEE transactions on pattern analysis and machine intelligence*, 2022. 5
- [20] Jungbeom Lee, Seong Joon Oh, Sangdoo Yun, Junsuk Choe, Eunji Kim, and Sungroh Yoon. Weakly supervised semantic segmentation using out-of-distribution data. In *Proceedings* of the IEEE/CVF Conference on Computer Vision and Pattern Recognition, pages 16897–16906, 2022. 5
- [21] Jungbeom Lee, Jihun Yi, Chaehun Shin, and Sungroh Yoon. Bbam: Bounding box attribution map for weakly supervised semantic and instance segmentation. In *Proceedings* of the IEEE/CVF conference on computer vision and pattern recognition, pages 2643–2652, 2021. 1
- [22] Minhyun Lee, Dongseob Kim, and Hyunjung Shim. Threshold matters in wsss: Manipulating the activation for the robust and accurate segmentation model against thresholds. In Proceedings of the IEEE/CVF Conference on Computer Vision and Pattern Recognition, pages 4330–4339, 2022. 5
- [23] Ruiwen Li, Zheda Mai, Zhibo Zhang, Jongseong Jang, and Scott Sanner. Transcam: Transformer attention-based cam refinement for weakly supervised semantic segmentation. *Journal of Visual Communication and Image Representation*, 92:103800, 2023. 1, 2, 4, 5, 6

- [24] Di Lin, Jifeng Dai, Jiaya Jia, Kaiming He, and Jian Sun. Scribblesup: Scribble-supervised convolutional networks for semantic segmentation. In *Proceedings of the IEEE conference on computer vision and pattern recognition*, pages 3159–3167, 2016. 1
- [25] Tsung-Yi Lin, Michael Maire, Serge Belongie, James Hays, Pietro Perona, Deva Ramanan, Piotr Dollár, and C Lawrence Zitnick. Microsoft coco: Common objects in context. In Computer Vision–ECCV 2014: 13th European Conference, Zurich, Switzerland, September 6-12, 2014, Proceedings, Part V 13, pages 740–755. Springer, 2014. 2
- [26] Chunmeng Liu, Guangyao Li, Yao Shen, and Ruiqi Wang. Mecpformer: Multi-estimations complementary patch with cnn-transformers for weakly supervised semantic segmentation. arXiv preprint arXiv:2303.10689, 2023. 2, 5
- [27] Jonathan Long, Evan Shelhamer, and Trevor Darrell. Fully convolutional networks for semantic segmentation. In *Proceedings of the IEEE conference on computer vision and pattern recognition*, pages 3431–3440, 2015. 1
- [28] Ilya Loshchilov and Frank Hutter. Decoupled weight decay regularization. arXiv preprint arXiv:1711.05101, 2017. 4
- [29] László Lovász. Random walks on graphs. Combinatorics, Paul erdos is eighty, 2(1-46):4, 1993. 2
- [30] Zhiliang Peng, Wei Huang, Shanzhi Gu, Lingxi Xie, Yaowei Wang, Jianbin Jiao, and Qixiang Ye. Conformer: Local features coupling global representations for visual recognition. In *Proceedings of the IEEE/CVF international conference on computer vision*, pages 367–376, 2021. 1, 2
- [31] Olga Russakovsky, Jia Deng, Hao Su, Jonathan Krause, Sanjeev Satheesh, Sean Ma, Zhiheng Huang, Andrej Karpathy, Aditya Khosla, Michael Bernstein, et al. Imagenet large scale visual recognition challenge. *International journal of computer vision*, 115:211–252, 2015. 1, 4
- [32] Yukun Su, Ruizhou Sun, Guosheng Lin, and Qingyao Wu. Context decoupling augmentation for weakly supervised semantic segmentation. In *Proceedings of the IEEE/CVF international conference on computer vision*, pages 7004–7014, 2021. 5
- [33] Ashish Vaswani, Noam Shazeer, Niki Parmar, Jakob Uszkoreit, Llion Jones, Aidan N Gomez, Łukasz Kaiser, and Illia Polosukhin. Attention is all you need. *Advances in neural information processing systems*, 30, 2017. 1
- [34] Yude Wang, Jie Zhang, Meina Kan, Shiguang Shan, and Xilin Chen. Self-supervised equivariant attention mechanism for weakly supervised semantic segmentation. In Proceedings of the IEEE/CVF conference on computer vision and pattern recognition, pages 12275–12284, 2020. 2, 5
- [35] Yunchao Wei, Jiashi Feng, Xiaodan Liang, Ming-Ming Cheng, Yao Zhao, and Shuicheng Yan. Object region mining with adversarial erasing: A simple classification to semantic segmentation approach. In *Proceedings of the IEEE conference on computer vision and pattern recognition*, pages 1568–1576, 2017. 2
- [36] Zifeng Wu, Chunhua Shen, and Anton Van Den Hengel. Wider or deeper: Revisiting the resnet model for visual recognition. *Pattern Recognition*, 90:119–133, 2019. 4
- [37] Lian Xu, Mohammed Bennamoun, Farid Boussaid, Hamid Laga, Wanli Ouyang, and Dan Xu. Mctformer+: Multi-class

token transformer for weakly supervised semantic segmentation. *arXiv preprint arXiv:2308.03005*, 2023. 2, 5

- [38] Lian Xu, Wanli Ouyang, Mohammed Bennamoun, Farid Boussaid, Ferdous Sohel, and Dan Xu. Leveraging auxiliary tasks with affinity learning for weakly supervised semantic segmentation. In *Proceedings of the IEEE/CVF international conference on computer vision*, pages 6984–6993, 2021. 5
- [39] Sung-Hoon Yoon, Hyeokjun Kweon, Jegyeong Cho, Shinjeong Kim, and Kuk-Jin Yoon. Adversarial erasing framework via triplet with gated pyramid pooling layer for weakly supervised semantic segmentation. In *European Conference* on Computer Vision, pages 326–344. Springer, 2022. 5
- [40] Dong Zhang, Hanwang Zhang, Jinhui Tang, Xian-Sheng Hua, and Qianru Sun. Causal intervention for weaklysupervised semantic segmentation. Advances in Neural Information Processing Systems, 33:655–666, 2020. 5
- [41] Fei Zhang, Chaochen Gu, Chenyue Zhang, and Yuchao Dai. Complementary patch for weakly supervised semantic segmentation. In *Proceedings of the IEEE/CVF international conference on computer vision*, pages 7242–7251, 2021. 2, 5
- [42] Bolei Zhou, Aditya Khosla, Agata Lapedriza, Aude Oliva, and Antonio Torralba. Learning deep features for discriminative localization. In *Proceedings of the IEEE conference on computer vision and pattern recognition*, pages 2921–2929, 2016. 1
- [43] Lianghui Zhu, Yingyue Li, Jieming Fang, Yan Liu, Hao Xin, Wenyu Liu, and Xinggang Wang. Weaktr: Exploring plain vision transformer for weakly-supervised semantic segmentation. arXiv preprint arXiv:2304.01184, 2023. 2